PHYSICAL REVIEW B, VOLUME 64, 165411

Electron affinity of plasma-hydrogenated and chemically oxidized diamond (100) surfaces

F. Maier, J. Ristein, and L. Ley*
Institut für Technische Physik, Universität Erlangen, Erwin-Rommel-Str. 1, D-91058 Erlangen, Germany

(Received 03 May 2001; published 5 October 2001)

The electron affinity (EA) χ of single crystal diamond (100) is determined as a function of hydrogen and oxygen coverage by a combination of work function and photoemission experiments. For the fully hydrogenated (100)-(2×1):H surface an EA of -1.3 eV and for the oxidized surface C(100)-(1×1):O $\chi=+1.7$ eV are obtained. These are the lowest and the highest electron affinities, respectively, ever reported for any diamond surface. The variation in χ with O and H coverage is well described by a simple dipole model provided that the depolarization is properly taken into account for high adsorbate densities. This analysis favors the bridge position (etherlike) for oxygen on C(100). By mixing H and O adsorbates on a microscopic scale the EA of C(100) can be adjusted at will over 3 eV between the extreme values without jeopardizing the chemical passivation of the diamond surface afforded by H or O termination.

DOI: 10.1103/PhysRevB.64.165411 PACS number(s): 73.30.+y, 81.05.Uw, 71.20.Mq

I. INTRODUCTION

Diamond exhibits considerable potential for applications on account of its outstanding mechanical and electronic properties (Ref. 1, and references therein). Especially, two features of diamond are unique among all semiconductors.[2] One is the true negative electron affinity (NEA) of the hydrogenated surface making diamond an efficient photoemitter and possibly a candidate in the field of cold cathode field emission.[3] Secondly, diamond shows under special circumstances a fairly high *p*-type surface conductivity which has already proven its potential for electronic devices.[4,5] As recently proposed by our group this latter property is closely related to the first one.[6] Within the framework of an electrochemical model a negative electron affinity of diamond of about -1.3 eV is a prerequisite for the observed surface conductivity. Therefore, quantitative information about the electron affinity of clean and adsorbate covered diamond surfaces is essential.

The electron affinity χ is the energy difference between the conduction band minimum E_{CBM} and the vacuum level E_{vac}

$$\chi=E_{\mathrm{vac}}-E_{\mathrm{CBM}}. \tag{1.1}$$

It can be modified by adsorbed surface atoms via the induction of a surface dipole layer. This situation is illustrated in the top part of Fig. 1 for the three surfaces of interest here. As hydrogen exhibits a lower electronegativity than carbon the C-H-bond is polarized with a positive charge δ^+ on the H atom. The ensuing double layer provides a potential step that pulls the vacuum level below the CBM over a distance that corresponds to the C-H bond length. By the same mechanism, adsorbates with a higher electronegativity than carbon raise χ compared to the clean surface as is the case for oxygen. The three surface configurations we are dealing with here are sketched at the bottom part of Fig. 1. The accepted model for the clean C(100) surface is a 2×1 reconstruction in the form of π-bonded dimers.[7,8] Upon hydrogenation the dimer C-C double bond is converted to a single bond with one H-atom attached to each carbon.[9] However, it is still under debate whether the (1×1) oxidized surface is the result of an ether-like (oxygen in bridge position) or a ketone-like (oxygen on top) geometry.[7]

Since the first report of NEA measurements on diamond by Himpsel and coworkers[10] a considerable number of publications have dealt with the electron affinity of bare and adsorbate-covered diamond surfaces. Salient experimental and theoretical results for the (111) and (100) surfaces of diamond are summarized in Table I. In all cases, χ is lowered by hydrogen and raised by oxygen relative to the bare surface. Nevertheless, absolute experimental values for the hydrogenated C(100) NEA surface are still missing. For C(111) single crystal diamond surfaces a detailed *in situ* study was performed by Cui *et al.* measuring simultaneously changes in work function and in band bending as a function of hydrogen coverage.[16] In this presentation we extend these investigations in a similar manner for the technologically more important (100) surface after hydrogenation and oxidation. These species are the principal adsorbates to be considered for diamond films synthesized by chemical vapor deposition (CVD)[19] and in electronic devices.[4] The electron affinity χ is derived from the absolute values of the work function ϕ and E_F-E_{VBM} (see Fig. 1) according to

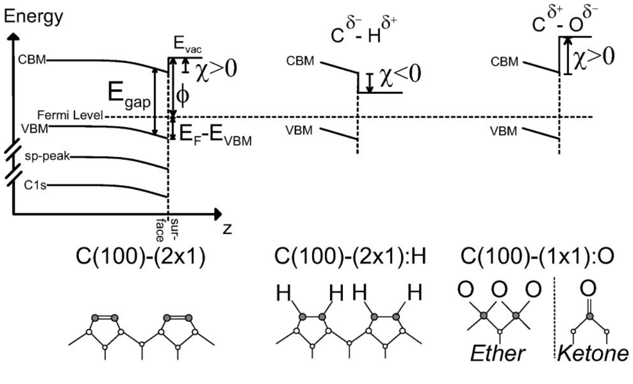

FIG. 1. Top: Band scheme and electron affinity χ for the bare, the hydrogenated, and the oxidized diamond (100) surface (for details, see text). Bottom: Sketch of the atomic arrangement of the bare, the hydrogenated and the oxidized (100) diamond surface.

TABLE I. Summary of electron affinities of clean, hydrogen and oxygen covered diamond surfaces. (sc: natural single crystal type IIb; homo: homoepitaxial boron doped CVD-film; HF-H *in situ* hydrogenation via hot filament; P-H/P-O: *ex situ* plasma hydrogenation/oxidation; UHV-A: Annealing in UHV).

Diamond	Sample Preparation	χ in eV	Reference
(111)-(2×1)	sc UHV-A	≈ 0.5	11
	sc UHV-A	0.5	14
	sc UHV-A(1000 K)	0.38	16
	sc UHV-A	1.5	15
(111)-(1×1):H	sc HF-H	$\leqslant -0.7$	11
	sc chem. oxidized, P-H	<0	14
	sc P-H	$\leqslant -0.9$	15
	sc P-H	-1.27	16
(111) graphitized	sc UHV-A(1400 K)	0.80	17
(111)-(2×1)	theory	0.35	18
(111)-(1×1):H	theory	-2.03	18
(100)-(2×1)	sc UHV-A	0.75	14
	sc UHV-A	1.3	15
	sc UHV-A	0.5	this work
(100)-(2×1):H	sc P-H	≈ -0.8	12
	sc HF-H	≈ -0.4	13
	sc P-H	$\leqslant -1.0$	15
	homo P-H	0.19	7
	sc P-H	-1.3	this work
(100)-(1×1):O	sc chem. oxidized	$\approx 1.0-1.5$	14
	homo P-O	≈ 0.64	7
	sc chem. oxidized	1.7	this work
(100)-(2×1)	theory	0.51	18
(100)-(2×1):H	theory	-2.05	18
(100)-(1×1): O_{ether}	theory	2.61	18
(100)-(1×1): O_{ketone}	theory	3.64	18

$$\chi = \phi + (E_F - E_{\text{VBM}}) - E_{\text{gap}}. \tag{1.2}$$

It will be shown that the electron affinity of diamond may vary from -1.3 eV for the fully hydrogenated C(100)-(2×1):H up to $+1.7$ eV for the oxidized C(100)-(1×1):O surface. This covers a range of about 3 eV for the same semiconductor. We are not aware of a comparable variability of electron affinities in any other semiconductor system.

II. EXPERIMENTAL

A. Sample preparation and temperature measurement

The sample used in this study is a type IIb natural single crystal diamond with polished (100) faces of 3×5 mm^2 size. The boron concentration of about 10^{16}cm^{-3} provides a bulk conductivity that is high enough to avoid charging problems during the photoemission and work function measurements. In order to obtain oxygen termination the sample is boiled for one hour in a solution of *conc.* HNO_3/H_2SO_4 (1:3) at 350 °C (Refs. 20, 21) after a preceding annealing step in UHV at 1100 °C that serves to remove residual chemisorbed hydrogen. For hydrogenation the acid treated surface is exposed to a microwave hydrogen plasma at about 800 °C for five minutes. This *ex situ* "surface polishing" treatment improves markedly the surface quality[22,23] and yields a diamond surface which is passivated by hydrogen.[24] Clamped to a tantalum foil the sample is heated from the back by electron bombardment in ultrahigh vaccum (UHV). At each thermal annealing step the temperature is controlled using an IR pyrometer that measures the temperature of the sample holder underneath the diamond. These are the temperatures given in the following. Comparing our values with typical desorption temperatures for hydrogen [$800-1000$ °C (Ref. 25)] the absolute surface temperature is estimated to be about $100-200$ °C lower than given by the IR pyrometer while the relative temperatures are measured with an accuracy of ±5 °C. The interpretation of our results does not depend on the absolute temperatures.

B. Surface characterization

At a base pressure of 10^{-10} mbar core-level spectroscopy (XPS) and valence-band spectroscopy (UPS) measurements are performed (combined energy resolution: $\Delta E_{\text{XPS}} \approx \pm 0.3$ eV, $\Delta E_{\text{UPS}} \approx \pm 0.04$ eV). All energies are measured relative to the common Fermi level E_F that is determined from a reference gold foil. From Eq. (1.2) the position of the VBM is required for the determination of χ. Since the

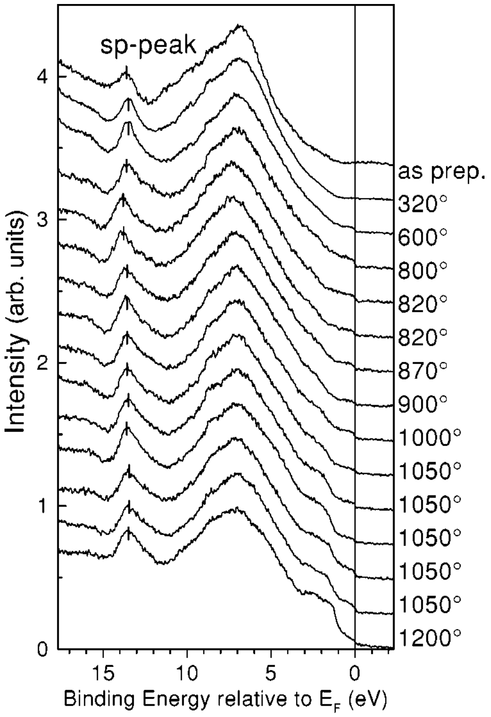

FIG. 2. Valence band spectra of the plasma hydrogenated (100) surfaces during thermal annealing in UHV ($\hbar\omega = 40.8$ eV, electron emission angle $\theta = 55°$).

VBM is not directly visible in UPS the energy distance of the VBM to experimental more accessible characteristic valence band features has been derived from an independent calibration experiment.[26] The energy distance of the VBM to the C1s core level in XPS and to the sp band[27] that gives rise to the sharpest valence band peak in UPS (called "sp peak") equals 283.9 and 12.80 eV, respectively, with an uncertainty of ± 0.1 eV.

Changes in work function are recorded as changes in the contact potential difference (CPD) between the diamond surface and a reference gold foil with an accuracy of ± 5 mV using the Kelvin method. The work function of the gold reference was independently determined *in situ* by total photoelectron yield spectroscopy following a procedure developed by Fowler.[28] The overall uncertainty in ϕ is thus ± 0.02 eV. Finally, changes in surface reconstruction are checked by low-energy electron diffraction (LEED).

III. RESULTS

A. Electron affinity of the plasma hydrogenated (100) surface

After acid treatment and hydrogen plasma exposure surface contaminants and oxygen are below the detection limit of XPS (≈ 0.1 monolayers). Furthermore, the LEED pattern reveals a (2×1) reconstruction with virtually no diffuse background intensity which is typical for a well-ordered, plasma hydrogenated (100) diamond surface. Figure 2 depicts selected valence band spectra during an annealing sequence from nominally 320 °C up to 1200 °C. From the average binding energy of the sp peak of 13.57 eV relative to E_F a position of the VBM of 0.77 eV below E_F was derived. With a bulk Fermi level at ≈ 0.4 eV above VBM for a boron doped diamond this corresponds to a downward band bending of 0.4 eV. At temperatures above 1000 °C a shoulder at 2 eV binding energy appears that is attributed to the formation of a surface state[8,29] which is characteristic for the clean surface. The small Fermi edge in the spectra of Fig. 2 has nothing to do with the sample itself. It originates from the tantalum clamps that are illuminated by a small fraction of the UV light. Below 600 °C the Ta is oxidized and exhibits no Fermi edge. In Fig. 3 $E_F - E_{\mathrm{VBM}}$ (open squares), the work function ϕ (open circles), and the electron affinity χ (filled squares) are plotted versus the accumulated annealing time t_A. Up to $t_A = 120$ min the temperature is raised in steps up to nominally 1000 °C. Beyond that point the temperature is kept constant at 1050 °C. Throughout the whole experiment the LEED pattern remained unchanged 2×1; after the final 1200 °C step the background intensity increased slightly indicating the beginning of surface graphitization. Moreover, the lateral extension of well-ordered domains was reduced significantly as witnessed by weak streaking of the half ordered spots. The *statistical* error in χ as determined by the uncertainty in the UPS and the CPD measurements is ± 0.04 eV; a *systematic* uncertainty of ± 0.1 eV originates mainly from the determination of the VBM relative to the sp peak.[26] From an initial value of -1.0 eV for the *as prepared* state χ decreases for the first annealing steps reaching a minimum of -1.3 eV at 400 °C and rises thereafter to -0.8 eV after 120 min of annealing. Starting the isothermal annealing sequence at 1050 °C the main change in electron affinity takes place until $\chi = +0.5$ eV. For the last heating step at 1200 °C a further increase of $+0.3$ eV is measured. Except for the initial value of χ for the *as prepared* surface, results similar to those of Fig. 3 have been reproduced several times.

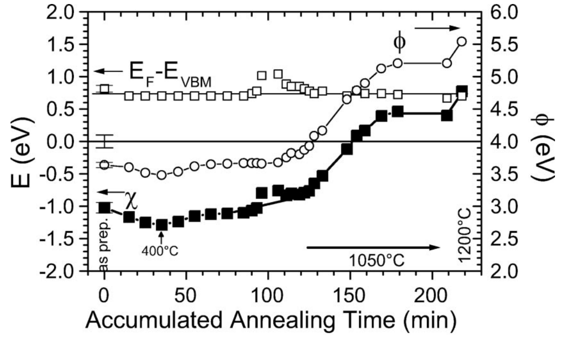

FIG. 3. Band bending $E_F - E_{\mathrm{VBM}}$ (open squares), work function ϕ (open circles), and electron affinity χ (filled squares) of the plasma hydrogenated (100) surface during the annealing sequence.

B. Electron affinity of the chemically oxidized (100) surface

A similar experiment as described in Sec. III A was performed for the chemically oxidized diamond (100) surface. After UHV annealing for complete dehydrogenation the sample is boiled in HNO_3 and H_2SO_4. LEED of the *as-prepared* surface shows a 1×1 pattern. In addition, very weak diffraction intensity is observed at the half-order spot

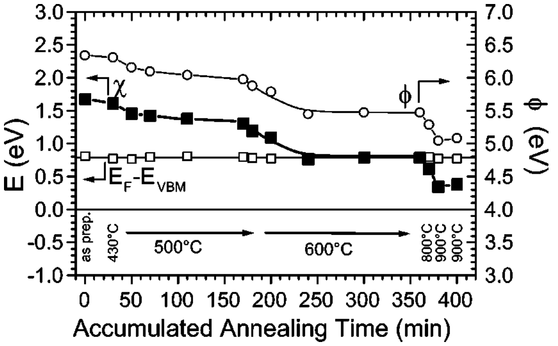

FIG. 4. Band bending $E_F - E_{\mathrm{VBM}}$ (open squares), work function ϕ (open circles) and electron affinity χ (filled squares) of the chemically oxidized (100) surface during the annealing sequence.

positions. During annealing the half-order spot intensities increase with a diffuse background intensity that is higher than for the hydrogenated (100) surface.

XPS reveals oxygen as the only adsorbate. $E_F - E_{\mathrm{VBM}}$ is taken from the C1s binding energy by subtracting 283.9 eV (see Sec. II B). As before, work function changes and band bending are monitored during annealing at different temperatures by Kelvin probe measurements and photoemission. Figure 4 summarizes the relevant quantities for the annealing sequence of the oxidized sample. No changes in band bending are observed up to nominally 900 °C with a VBM position of about 0.8 eV below E_F which is virtually identical to that of the hydrogenated sample. From the CPD measurements the work function ϕ starts to decrease from 6.3 eV within the 500 °C isothermal annealing sequence. This trend is accelerated at 600 °C until ϕ reaches a value of 5.5 eV. At higher temperatures (800 and 900 °C) ϕ drops to its final value of 5.1 eV. On the basis of Eq. (1.2) the electron affinity χ follows this behavior dropping from its initial value of $+1.7$ eV down to $+0.4$ eV.

IV. DISCUSSION

Throughout all the experiments the pinning of the surface Fermi level at about 0.8 eV above VBM was unexpected. Experiments reported by other groups[11,30] and performed on other (100) samples by us show that hydrogen adsorption and desorption may indeed influence the Fermi level position at the surface. Typical values of $E_F - E_{\mathrm{VBM}}$ between 0.3 and 1 eV have been observed.[30] The different behavior of our sample used in this study is possibly due to *extrinsic* graphitelike defects located in the near surface region which are not removed by the hydrogen plasma or the acid treatment. For a weakly *p*-doped diamond as used in our case a graphite content of 0.1% of the surface is sufficient to pin the Fermi level between 0.7 and 0.8 eV above VBM.[2]

Before partial graphitization of the hydrogenated surface occurs as indicated by LEED above nominally 1100 °C the saturation value of $\chi = +0.5$ eV is that of the clean (100)-(2×1) surface. This is in good agreement with theoretical predictions (see Table I). However, higher values of $+0.75$ eV (Ref. 14) and in particular $+1.3$ eV (Ref. 15) are derived by others from the width of valence band photoemission spectra. As mentioned in the preceding section, the determination of the VBM with an accuracy better than 0.2 eV is difficult in UPS. In addition, a reliable value for the vacuum level is difficult to obtain from the low energy cutoff of the spectra because the spectral shape depends sensitively on the analyzer characteristic in this regime. Whether the higher values reported for the clean surface are thus due to experimental deficiencies or to different surface treatments is hard to say. When graphitization occurs after the 1200 °C step χ increases by an additional 0.3 eV. This situation is identical for the graphitized (111) diamond surface where a value of $\chi = +0.80$ eV was observed.[17]

The initial value of χ of the plasma hydrogenated surface varies between -1.0 eV (Fig. 3) and -0.6 eV after nominally identical preparation conditions. However, the minimum value $\chi_{\mathrm{min}} = -1.3$ eV after 400 °C annealing in UHV has been confirmed several times. In this temperature range, airborne hydrocarbon contaminations are known to desorb as reported by Graupner *et al.*[31] We therefore attribute χ_{min} to the contaminant-free C(100)-(2×1):H surface, a value that is virtually identical to that of C(111)-(1×1):H.[16] Hence, the dipole-induced change $\Delta\chi$ (see Fig. 1) of 1.8 is 0.1 eV larger for C(100) than for C(111) (Table I). According to the lower surface carbon density and the tilt-angle of about 25° (Ref. 9) of the C-H bonds the dipole density is about 20% lower on C(100) compared to C(111). Within the simplest electrostatic model of independent dipoles one would thus expect the same 20% difference in $\Delta\chi$ of the two surface orientations. However, this is partially compensated by a smaller depolarization influence of adjacent C-H-dipoles at the less dense (100) surface as seen in the following.

The dipole-induced lowering of χ is expressed by the areal density n of the C-H dipoles and their projected dipole moment p_z (Ref. 32) according to

$$\chi = \chi_0 - \frac{e}{\epsilon_0} p_z n f(n). \tag{4.1}$$

Here, z is the direction perpendicular to the surface, ϵ_0 the dielectric constant of free space, and e the elementary charge, respectively. The function $f(n)$ accounts for the depolarization effects. In the mutual field $\underline{E}$ of all dipoles the individual dipole moment

$$\underline{p} = \underline{p}_0 - \underline{\alpha}\ \underline{E} \tag{4.2}$$

is reduced from its value $\underline{p}_0$ at infinite dipole dilution by the bond polarizability $\underline{\alpha}$ which is a tensor in general. In the case of a square or hexagonal plane network of perpendicular oriented dipoles Topping[33] derived a simple expression for $f(n)$ as

$$f(n) = \left(1 + \frac{9}{4\pi\epsilon_0} \alpha n^{1.5}\right)^{-1}, \tag{4.3}$$

where α is the polarizability along the dipole axis and thus a scalar. With Eq. (4.3) the dependence of χ with hydrogen coverage was successfully evaluated for the C(111) surface.[16] As a first approximation, Eq. (4.3) was also used for the (100) configuration though the real geometry differs

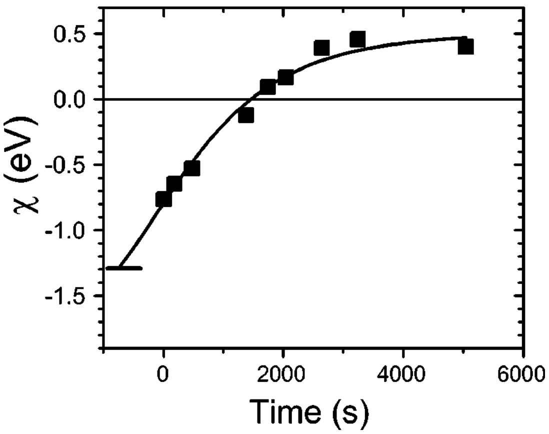

FIG. 5. Electron affinity χ versus annealing time at 1050 °C during hydrogen desorption; the solid line is a fit to the data points with a dipole moment $p_z = 0.08$ e Å and a polarizability $\alpha = 1.0 \times 10^{-30}$Asm^2/V (see text).

from that assumed by Topping. The solid line in Fig. 5 is a fit to the isothermal annealing sequence at 1050 °C of Fig. 3 according to Eqs. (4.1) and (4.3). Assuming first order desorption kinetics of hydrogen from diamond (100) (Ref. 34) the H coverage $n(t_A) = n_0 e^{-\nu t_A}$ where n_0 equals the surface density of carbon atoms of 1.57×10^{15}cm^{-2} at $\chi = -1.3$ eV and t_A the annealing time. The desorption rate ν and the initial coverage $n(t=0)$ are fit parameters. The derived C-H dipole moment of $p_z = 1.32 \times 10^{-30}$ Asm^2/V (0.08 e Å) is 10% lower than on the hydrogenated C(111) surface as expected on account of the tilt angle. However, agreement with experiment requires a polarizability α of 1.0×10^{-30} Asm^2/V which is about 30% lower than that given by Cui *et al.* for C(111)-(1×1):H.[16] This is not unreasonable because the polarization of the C-H bond is certainly smaller for any direction that does not coincide with the bond axis. Hence, the depolarization perpendicular to the surface that is considered in Eq. (4.3) is smaller for the (100) than for the (111) configuration on account of the tilted C-H axis on the former surface. Our findings corroborate *ab initio* calculations of Robertson *et al.* (Ref. 18 in Table I). They also predict a larger variation of χ between the clean and the hydrogen terminated C(100) surface compared to C(111).

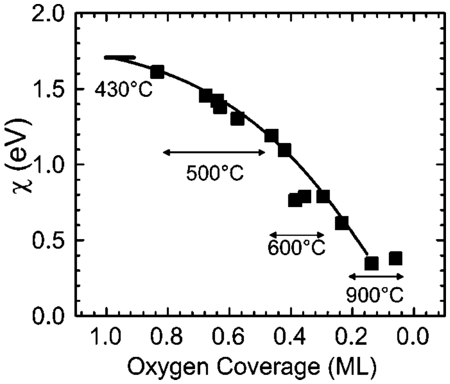

FIG. 6. Electron affinity χ versus oxygen coverage; the solid line is a fit to the data with a dipole moment $p_z = -0.10$ e Å and a polarizability $\alpha = 2.0 \times 10^{-30}$Asm^2/V (see text).

The analysis for the oxidized sample differs from the hydrogenated case in that a direct correlation between changes in χ and oxygen coverage is possible. The latter is obtained with an accuracy of about 10% from the ratio of the O1*s* to the C1*s* intensities taking the different cross sections for photoionization[35] and the effective sampling depth of 9 Å (Ref. 36) into account. The initial oxygen coverage after the acid treatment corresponds to nominally 1.4 monolayer (ML). After a 430 °C annealing step the oxygen coverage has dropped to about 0.8 ML. However, the oxygen that is directly bonded to diamond did not change during the first annealing step. This part of oxygen gives rise to a C1*s* component in XPS that is shifted by 2.5 eV towards higher binding energies relative to the C1*s* level of bulk diamond and it remains unaffected up to 430 °C annealing. We therefore ascribe the desorbed oxygen fraction to a water layer that is present after the acid treatment. This is in keeping with the observation that χ does not change after this annealing step if we assume the water molecules to be randomly oriented at the surface. During the following annealing steps the O1*s* and the chemically shifted C1*s* component decrease in the same proportion. Consequently, the correlation between oxygen coverage and χ in Fig. 6 starts after the 430 °C step. The solid line in Fig. 6 is a fit to the experimental values of χ according to Eqs. (4.1) and (4.3) yielding a perpendicular dipole moment $p_z = -0.10$ e Å of the C-O bonds and a polarizability $\alpha = 2 \times 10^{-40}$ Asm^2/V that is close to the polarizibility of carbon monoxide [2.2×10^{-40} Asm^2/V (Ref. 37)]. Based on the Pauling electronegativities[38] of carbon (2.55) and oxygen (3.44) a charge transfer Δq of 0.17e is estimated, and thus our measured dipole moment corresponds to a thickness of the C-O-dipole layer of 0.6 Å. This is in excellent agreement with LEED-IV studies by Wang and co-workers.[7] They find on thermally oxidized (100) surfaces a C-O layer spacing of 0.7 Å where the oxygen occupies the bridge position (ether configuration in Fig. 1). A comparison of our experimental values of χ with the theoretical results of Robertson and Rutter[18] (Table I) also indicates that the bridge place of the chemically oxidized (100) surface is favored. Scaling the calculated electron affinity differences $\Delta\chi_{\text{theory}}$ between the clean and the hydrogenated (100) and (111) surfaces by the factor 0.7 to fit the experimental values of this work and that of Cui *et al.*[16] the theoretical values provide an electron affinity of +2.0 eV for the (100)-(1×1): O$_{\text{ether}}$ surface and +3.0 eV for the (100)-(1×1): O$_{\text{ketone}}$ geometry. Thus, our experimental value of $\chi = +1.7$ eV clearly favors bridge oxygen as bonding configuration. Extrapolating the fit curve of Fig. 6 to zero oxygen coverage one may deduce an electron affinity of the bare surface of about 0 eV. This is considerably lower than the 0.5 eV obtained after hydrogen desorption and we conclude that the acid treatment does leave some residual hydrogen chemisorbed at the surface which lowers the electron affinity by an offset of 0.5 eV throughout the whole annealing sequence. For that reason χ increases again at the last 900 °C step when hydrogen starts to desorb simultaneously with oxygen (Fig. 4). This finding is supported by the LEED pattern that exhibits from the beginning very weak diffraction intensity at the half order spot positions and which are characteristic for the hydrogenated (100) surface. Consequently, a fully oxidized (100) surface should have an electron affinity of 2.2 eV which also agrees better with the theoretical value of 2.0 eV discussed above in the case of the ether configuration. For reasons that are not clear at the moment, we never achieved such a high value in any of our experiments.

Finally, it should be mentioned that the chemical oxidation works quite effectively on the plasma hydrogenated surface as well. After plasma treatment ($\chi=-0.7$ eV) and mild annealing to desorb hydrocarbons ($\chi=-1.3$ eV) the sample was removed from UHV and boiled in acid for half an hour. The resulting electron affinity of $+1.2$ eV proved a partial oxidation of the surface. Therefore, it should be possible to adjust quasicontinuously the electron affinity of the (100) diamond. Starting from the hydrogenated surface a large variation of χ from -1.3 up to 1.7 eV by the use of controlled oxidation parameters (time, temperature, acid concentration, etc.) offers a simple way to manipulate χ-related properties such as surface conductivity, Schottky barrier heights, and onset-field in field emission.

V. SUMMARY

By studying the diamond (100) surface with photoemission and work function measurements we were able to determine values of the electron affinity of the clean C(100)-(2×1) ($+0.5$ eV) and the hydrogenated C(100)-(2×1):H (-1.3 eV) surface with an accuracy of ±0.1 eV. Initial contamination by physisorbates (most probably hydrocarbons) increase the electron affinity by a few tenths of electron volts compared to the mildly annealed, and thus contamination-free hydrogenated surface. The measured electron affinity of the chemically oxidized C(100) of $+1.7$ eV represents a lower limit for a purely oxidized (100)-(1×1):O diamond surface because residual hydrogen provided by the acid treatment could not be avoided. This value of χ is only compatible with a bridge-site occupation of oxygen (ether-configuration) on the (100) surface. An analysis of the electron affinity in the framework of adsorbate induced dipole layers shows good agreement with experimental findings when depolarization effects are taken into account. From the change of χ during thermal annealing vertical dipole moments of the C-H ($\approx 0.08\ e$ Å) and the C-O ($\approx -0.10\ e$ Å) bonds are derived.

For all (100) surfaces examined here, the surface Fermi level is pinned $+0.8$ eV above the valence band maximum. The origin of the defect states that are required to fix E_F at the surface lies most probably in the mechanical polishing processes of the sample.

ACKNOWLEDGMENTS

We thank M. Stammler for the microwave plasma preparation. The authors gratefully acknowledge financial support by the Deutsche Forschungsgemeinschaft (Project No. Le 643/5-3).

---

*Corresponding author; E-mail address: Lothar.Ley@physik.uni-erlangen.de

[1] *Springer Series in Materials Processing: Low-pressure Synthetic Diamond*, edited by B. Dischler and C. Wild (Springer, Berlin, 1998).

[2] J. Ristein, F. Maier, M. Riedel, J.B. Cui, and L. Ley, Phys. Status Solidi A **181**, 65 (2000).

[3] M.W. Geis and J.C. Twichell, Appl. Phys. Lett. **67**, 1328 (1995).

[4] P. Gluche, A. Aleksov, W. Ebert, and E. Kohn, IEEE Electron Device Lett. **18**, 547 (1997).

[5] K. Tsugawa, K. Kitatani, H. Noda, A. Hokazono, K. Hirose, M. Tajima, and H. Kawarada, Diamond Relat. Mater. **8**, 927 (1999).

[6] F. Maier, M. Riedel, B. Mantel, J. Ristein, and L. Ley, Phys. Rev. Lett. **85**, 3472 (2000).

[7] Y.M. Wang, K.W. Wong, S.T. Lee, M. Nishitani-Gamo, I. Sakaguchi, K.P. Loh, and T. Ando, Diamond Relat. Mater. **9**, 1582 (2000).

[8] R. Graupner, M. Hollering, A. Ziegler, J. Ristein, L. Ley, and A. Stampfl, Phys. Rev. B **55**, 10 841 (1997).

[9] J. Furthmüller, J. Hafner, and G. Kresse, Phys. Rev. B **53**, 7334 (1996).

[10] F.J. Himpsel, J.A. Knapp, J.A. van Vechten, and B.E. Eastman, Phys. Rev. B **20**, 624 (1979).

[11] C. Bandis and B.B. Pate, Phys. Rev. B **52**, 12 056 (1995).

[12] C. Bandis and B.B. Pate, Surf. Sci. **350**, 315 (1996).

[13] T.P. Humphreys, R.E. Thomas, D.P. Malta, J.B. Posthill, M.J. Mantini, R.A. Rudder, G.C. Hudson, R.J. Markunas, and C. Pettenkofer, Appl. Phys. Lett. **70**, 1257 (1997).

[14] P.K. Baumann and R.J. Nemanich, Surf. Sci. **409**, 320 (1998).

[15] L. Diederich, O.M. Küttel, P. Aebi, and L. Schlapbach, Surf. Sci. **418**, 219 (1998).

[16] J.B. Cui, J. Ristein, and L. Ley, Phys. Rev. Lett. **81**, 429 (1998).

[17] J.B. Cui, J. Ristein, and L. Ley, Phys. Rev. B **59**, 5847 (1999).

[18] J. Robertson and M.J. Rutter, Diamond Relat. Mater. **7**, 620 (1998).

[19] P.K. Bachmann, D. Leers, and H. Lydtin, Diamond Relat. Mater. **1**, 1 (1991).

[20] T. Ando (private communication).

[21] P.E. Phersson and T.W. Mercer, Surf. Sci. **460**, 49 (2000).

[22] B.D. Thoms, M.S. Owens, J.E. Butler, and C. Spiro, Appl. Phys. Lett. **65**, 2957 (1994).

[23] O.M. Küttel, L. Diederich, E. Schaller, O. Carnal, and L. Schlappach, Surf. Sci. **337**, L812 (1995).

[24] J. Ristein, W. Stein, and L. Ley, Phys. Rev. Lett. **78**, 1803 (1997).

[25] R.E. Thomas, R.A. Rudder, and R.J. Markunas, J. Vac. Sci. Technol. A **10**, 2451 (1992).

[26] F. Maier, R. Graupner, M. Hollering, L. Hammer, J. Ristein, and L. Ley, Surf. Sci. **443**, 177 (1999).

[27] Ralf Graupner, Ph.D. thesis, Universität Erlangen-Nürnberg, 1997.

[28] R.H. Fowler, Phys. Rev. **38**, 45 (1931).

[29] G. Francz and P. Oelhafen, Surf. Sci. **329**, 193 (1995).

[30] L. Diederich, O.M. Küttel, E. Schaller, and L. Schlapbach, Surf. Sci. **349**, 176 (1996).

[31] R. Graupner, F. Maier, J. Ristein, L. Ley, and Ch. Jung, Phys. Rev. B **57**, 12 397 (1998).

[32] E.V. Albano, Applic. Surf. Sci. **14**, 183 (1982).
[33] J. Topping, Proc. R. Soc. London, Ser. A **114**, 67 (1927).
[34] K. Bogrov, H. Shechter, M. Folman, and A. Hoffman, Diamond Relat. Mater. **7**, 170 (1998).
[35] J. J. Yeh, *Atomic Calculation of Photoionization Cross-Sections and Asymmetry Parameters* (Gordon and Breach Science Publishers, Langhorne, 1993).
[36] S. Hüfner, *Photoelectron Spectroscopy, Springer Series in Solid-State Science* Vol. 82 (Springer, Berlin 1995).
[37] *Handbook of Chemistry and Physics*, edited by R.C. Weast (CRC Press, Boca Raton 1978).
[38] W. Mönch, *Semiconductor Surfaces and Interfaces* (Springer, Berlin, 1995).